RSC Advances

Volume 1 | Number 1 | Jan 2013 | Pages 1–100

RSC Advances

www.rsc.org/advances

ROYAL SOCIETY OF CHEMISTRY

ROYAL SOCIETY OF CHEMISTRY

www.rsc.org/advances

Novel Ferrocene-based Nanoporous Organic Polymers for Clean Energy Application

Qingquan Liu[a*], Zhe Tang[a], Minda Wu[a], Bo Liao[a], Hu Zhou[a], Baoli Ou[a], Yu Guipeng[b], Zhihua Zhou[a*], Xiaojuan Li[a]

[a)] School of Chemistry and Chemical Engineering, Key Laboratory of Theoretical Chemistry and Molecular Simulation of Ministry of Education, Hunan University of Science and Technology, Xiangtan 411201, China

[b)] Key Laboratory of Resources Chemistry of Nonferrous Metals Ministry of Education, College of Chemistry and Chemical Engineering, Central South University, Changsha 410083, China

E-mail: (*qqliu@hnust.edu.cn; *zhou7381@126.com)

Abstract: A novel ferrocene-based nanoporous organic polymer (FNOPs-1) for clean energy application has been prepared by coupling 1,1'-ferrocene-dicarboxaldehyde with melamine. The BET surface area and the total pore volume of FNOPs-1 are 752.4 m^2/g and 1.32cm^3/g, respectively. FNOPs-1 exhibits excellent gas storage capacity like 16.61wt% of carbon dioxide, 3.48 wt% of methane, and 1.27 wt% of hydrogen at 273K/1.0bar.

The dramatic increases in the amount of greenhouse gases such as CO_2 and CH_4 in atmosphere are believed to be responsible for global warming, sea level rise, and climate change. Hydrogen is recognized as the cleanest energy source nowadays since combustion of hydrogen has high caloric value and environmentally compatible byproduct. In addition, methane is the main component of natural gas and at present, there is a great interest in expanding its application for fueling automobiles because of its widely availability and its lower CO_2 emission in comparison with petroleum. However, a current challenge for the development of hydrogen-based and methane-based technology is the available materials, which can store and deliver large amount of hydrogen or methane near room temperature and at low pressures.[1] In the past two decades, various porous polymers such as covalent organic frameworks (COFs),[2, 3] conjugated microporous polymers (CMPs),[4, 5] polymer with intrinsic microporosity (PIMs),[6] hypercrosslinked polymers (HCPs),[7, 8] and nanoporous organic polymers (NOPs)[9-11] were developed as adsorbents for gas storage and gas selective separation. As an emerging solid adsorbent, NOPs has attracted extensive interests and hold the greatest potential for commercial use due to a series of advantages like high porosity, low density, and excellent stability.[12-14] Recently, NOPs with functional building units was intensively investigated to obtain high gas storage capacity.[15]

Ferrocene and its derivatives are a kind of special organic metal complexes and have extensive applications in the field of electric catalytic and biological sensors.[16] To date, there are very few reports about the preparation and the application of ferrocene-based nanoporous frameworks.[17, 18] Weber and Kistan[17] prepared microporous ferrocenyl Schiff base network with a BET surface area of 430m^2/g by the coupling of 1,1'-diacetyl ferrocene with melamine. Recently, Ferrocene-based statistical copolymers of poly(ferrocenyl)-co-divinylbenzene produced by Kleitz et al.[18] showed porous properties with BET surface areas ranging from 385 to 899 m^2/g and hydrogen uptake of 0.4─0.67 wt%. Ferrocene possesses a double-deck sandwich structure, which can be used as a rigid building unit to expanded porosity of NOPs. Therefore, it would be valuable to use ferrocene derivatives as a building unit for NOPs and endow NOPs with new properties and application prospects.

Inspired by the above works, the strategy of ferrocene being a building unit of NOPs was demonstrated. We synthesized a novel ferrocenyl nanoporous organic polymer (FNOPs-1) by the coupling of 1,1'-ferrocenedicarboxaldehyde and melamine in the medium of dimethyl sulfoxide (DMSO) at 180℃, and investigated its gas uptake capacity. Scheme 1 shows the synthesis route of FNOP-1.

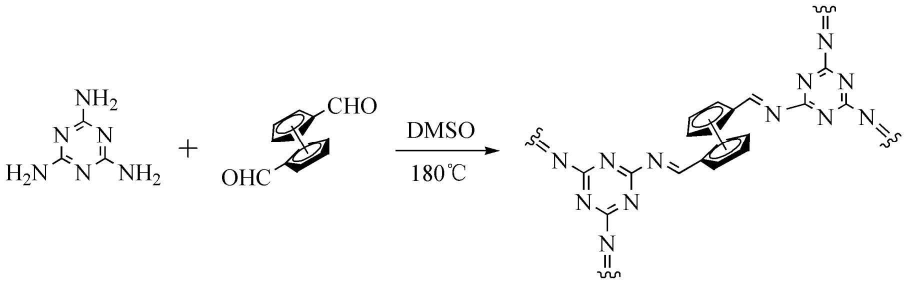

Scheme 1 Synthesis route to FNOPs-1

The synthesized FNOPs-1 was insoluble in any common organic solvent such as DMSO, N,N'-dimethylformamide (DMF), and tetrahydrofuran (THF), as well as in diluted HCl solution (~10 wt%). There was no weight loss can be found after soaked in diluted acid for 48 h, moreover, the BET surface area value of acid soaked FNOPs-1 was very close to that of the original FNOPs-1. These facts suggested that FNOPs-1 has a hypercrosslinked and physicochemical stable property. The thermal stability of FNOPs-1 was investigated by thermogravimetric analysis under air atmosphere (Fig. 1). The result indicated that FNOPs-1 remains stable up to approximately 240℃ (sharp weight loss) in air atmosphere, and the weight loss below 240℃ (0~20 wt%) was believed to be water and residual solvent loss due to smooth curve in the range of room temperature to 240℃. The strong charge transfer interactions between ferrocene and triazine rings were possibly responsible for its excellent thermal stability. The physicochemical and thermal stability of FNOPs-1 was comparable to that of other microporous polymer materials such as CMPs,[19] HCPs,[20] COFs,[3] and PIMs.[6] Furthermore, the thermal stability of FNOPs-1 is better than that of MOFs.[21] The excellent stability endows FNOPs-1 with broader application range, especially in a harsh environment.

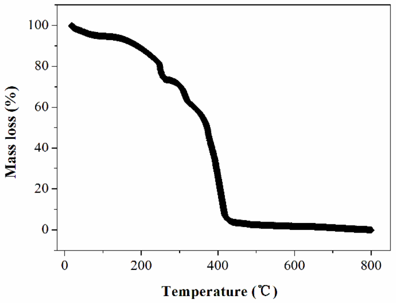

Fig. 1 TGA curves of FNOPs-1 under air atmosphere

The chemical structure of FNOPs-1 is firstly confirmed by solid-state 13C NMR spectroscopy. As shown in Fig.2, the spectrum shows four resonances at 113, 134, 163 and 177 ppm. The resonance at 113 ppm and 134 ppm can be assigned to the beta-C and the alpha-C atoms in ferrocene, respectively. The signal at 163ppm originates from the CH of C=N bond, which is slightly larger than that reported by Yaghi et al.[22] We think that the withdrawing electron effect of ferrocene will be responsible for that. The resonance at 177ppm can be correlated to the quaternary carbon atoms in the melamine, and is also slightly larger than the data reported by Müllen et al.[23] Apart from the above reason, the overlapping peaks of 163ppm and 177 ppm may be also the second reason for the large chemical shift.

The chemical structure of FNOPs-1 is characterized by Fourier tansform infrared (FT-IR). The FT-IR spectrum of FNOPs-1 (Figure S2) exhibits a characteristic stretching vibration of C=N at 1552 cm^{-1}. As for the C=N stretch band, there were several different reports like 1635cm^{-1},[24] 1620cm^{-1},[22] and 1597cm^{-1}.[25] In the present study, we think that the bond length of C=N was prolonged to accommodate ferrocene with double sandwich structure to achieve the most stable state. The prolonged bond length induced the red shift of C=N stretch band, and the increased absorbance strength in comparison with those reported in the early study.[24,25] Meanwhile, the stretching vibration of N-H in melamine at 3300-3500 cm^{-1} and C=O in 1,1'-ferrocenedi-carboxaldehyde at 1680 cm^{-1} have disappeared in the spectrum of FNOPs-1. Based on these experimental results, it can be concluded that melamine and 1,1'-ferrocenedicarboxaldehydethe are successfully coupled to form an organic network. Fig. 2A shows SEM image of FNOPs-1, and aggregated particles with random shape and sizes of 0.8–1.1 μm can be observed. AFM image (Fig. 2B) displays that FNOPs-1 is of porous and amorphous structure. In comparison with the raw materials of melamine, broad powder X-ray diffraction pattern of FNOPs-1 is featureless, suggesting its amorphous nature (Figure S4).

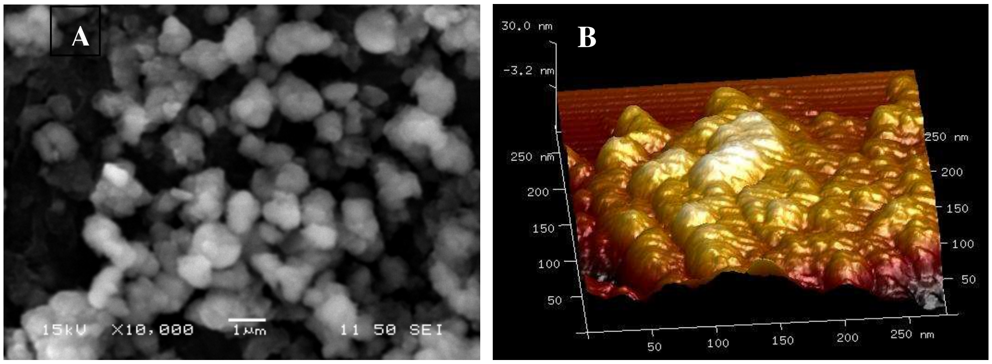

Fig. 2 SEM image of FNOPs-1

Nitrogen physisorption measurement is performed at 77K (Fig. 3A) in order to evaluate the pore structure of FNOPs-1. FNOPs-1 is microporous and exhibits a reversible Type-IV profile. There are a rapid uptake in the range of P/P_o= 0.05–0.15, indicative of numerous micropores in FNOPs-1, and a rapid uptake in the high pressure region (P/P_o= 0.6–0.9), suggesting that there are both mesoporous and macroporous structure in FNOPs-1. We think the voids derived from loose packing of small particles can be responsible for the macropores. It should be noted that there is a small adsorption-desorption hysteresis loop at high pressure region, which may be originated from the pore networks effect and also from the irreversible binding of nitrogen molecules to the pore surface. The Brunauer–Emmett–Teller surface area (S_{BET}) of FNOPs-1 was calculated to be 752.4 m^2g^{-1}, and the total pore volume of 1.32 cm^2/g. Although the surface area is lower than those of most COFs[2, 26] and MOFs,[27, 28] the total pore volume is still higher than that of COFs,[26, 29] CMPs,[30, 31] and other porous polymer materials.[8, 32]

Pore size distribution curves of FNOPs-1 are estimated from the nitrogen adsorption branch by the nonlocal density functional theory (NLDFT) and shown in Fig. 3B. The data show a large number of pores in the micropore region extending to a more significant mesopore population. However, NLDFT fails to calculate the macropore fraction at all. The pore size distribution curve got from BJH method (Figure S5) exhibits a lower fraction of macropore.

Up to now, it is still a considerable challenge for onboard storage of H_2 and CH_4 fuels to meet volumetric and gravimetric targets in automotive applications, and it is also necessary to develop CO_2 capture and sequestration technologies for stabilizing atmospheric CO_2 levels. The remarkable porosity of FNOPs-1 intrigues us to investigate their performance in gas storage under low pressure conditions. Low pressure H_2, CH_4, and CO_2 isotherms of FNOPs-1 are provided in Figure 3C-E, respectively. Moderate hydrogen storage (142.5 cm^3/g, 1.27 wt%) is observed for FNOPs-1 at 77 K/1.0 bar, and under these conditions, H_2 isotherms are not fully saturated because of the low critical temperature of H_2 (33 K).[1] This data is comparable to those of many other reported organic polymer networks such as ILCOF-1,[3] CTC-COF,[33] CPF-103,[1] TzF-7,[15] and NOPs,[9, 10] as well as ferrocenyl hyper-cross-linked polymer PFe,[18] although the S_{BET} of FNOPs-1 is lower than those of the porous organic polymers. Kleitz and Morin et al.[18] also demonstrated that small amount of ferrocenyl units could significantly increase the hydrogen adsorption capacity of hyper-cross-linked polymers. A small hysteresis suggests that there is an interaction between H_2 and the pore surface of FNOPs-1, which is possibly responsible for the excellent hydrogen uptake capacity of FNOPs-1.

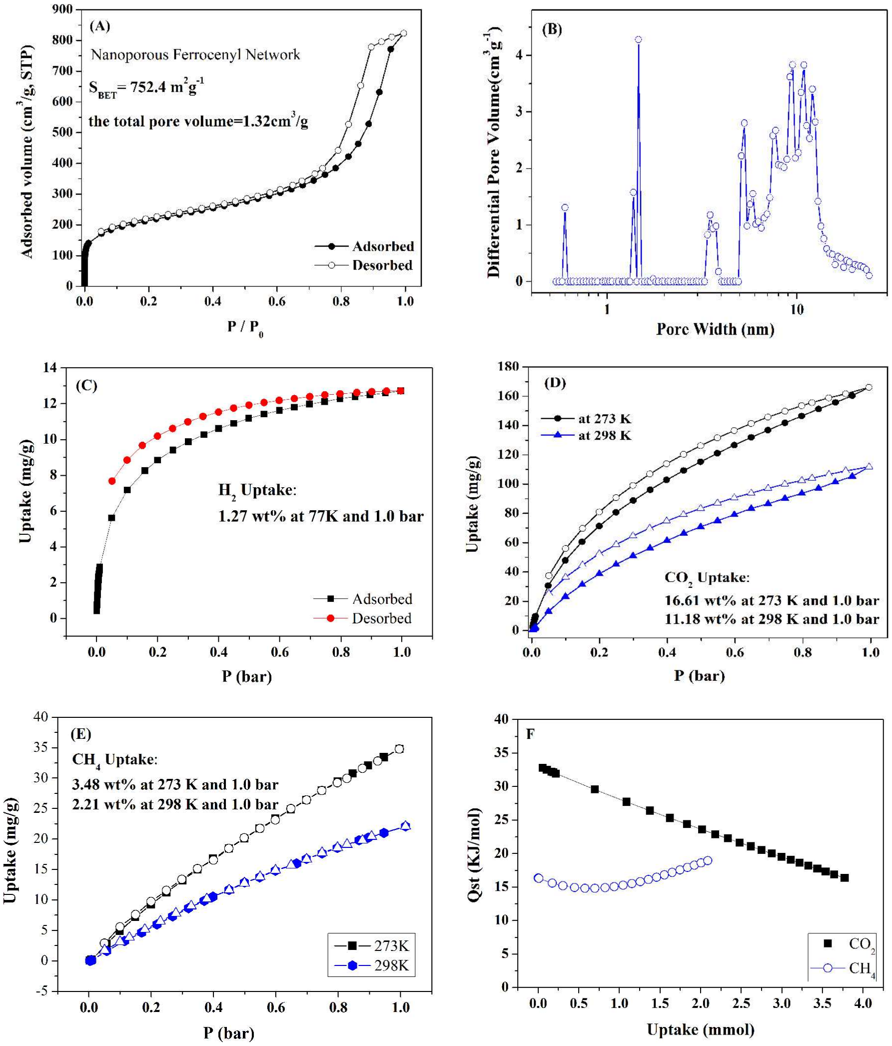

Fig. 3 Gas sorption measurements of FNOPs-1: A) N_2 isotherm curves, B) pore-size distribution curves derived from NLDFT, C) H_2, D) CO_2, E) CH_4, and F) Isosteric heats of adsorption of CO_2 and CH_4 for FNOPs-1 at different loadings.

The CO_2 adsorption and desorption isotherms for FNOPs-1 were collected at 273K and 298K and presented in Fig. 3D. FNOPs-1 exhibited a respectable CO_2 uptake capacity of 16.61 wt% (84.6 cm^3/g) at 273K/1bar and 11.18 wt% (56.9 cm^3/g) at 298K/1bar, respectively. These data were much higher than most of the previously reported nanoporous organic polymers with ultrahigh BET surface area such as BLPs (12.8wt%, 2866 m^2g^{-1}),[34] TDCOF-5 (9.2 wt%, 2497 m^2g^{-1}),[35] and ILCOF-1 (6.0wt%, 2723 m^2g^{-1}) under similar condition of 273K and 1.0 bar, but are lower than those of CPOP-1 (21.2 wt%, 2220 m^2g^{-1})[36] and SUN-C1-sca (19.3 wt%, 830 m^2g^{-1}).[37] The characteristics for CO_2 uptake on FNOPs-1 were considered to be attributed to two factors. The first factor is the interaction between ferrocene units and CO_2 molecules, because ferrocene is of withdrawing electron property and carbon dioxide is electron-rich, thus enhancing the CO_2 adsorption property. The second factor is the interaction sites provided by heteroatoms in FNOPs, which can enhance CO_2 adsorption properties through dipole-dipole interaction.[38] The small hysteresis in the CO_2 adsorption and desorption isotherms demonstrated the interaction between CO_2 and the solid surface.

In order to understand these observations, the coverage-dependent isosteric heats of CO2 adsorption (Q_{st}) for FNOPs-1 were calculated from the CO_2 adsorption branches at 273K and 298K by the Virial method[39] (Figure S6A). As shown in Fig. 3F, the adsorption enthalpy is 32.8 KJ/mol at the onset of adsorption, indicating a strong CO_2-FNOPs-1 interaction, and gradually decreases to 16.37 KJ/mol with increasing the adsorption amount to 3.77 mmol/g. The value exceeds those reported for similar porous polymers like imine-linked COFs (18.3 KJ/mol)[3] and CPOP-1(27KJ/mol),[36] and is comparable to those of the functionalized porous polymers such as CMP-1-COOH (32.6 kJ/mol),[40] PPN-6-SO_3H (30.4 kJ/mol) and PPN-6- SO_3Li (35.7 kJ/mol).[41] However, it is should be noted that the value of adsorption heat remain much below the energy of the chemical bond, suggesting the strong physisorption, which is desirable for CO_2 release.

The CH_4 isotherms at 273K and 298K are shown in Fig. 3E. The methane uptake of FNOPs-1 increases with an increase in the pressure, and achieves 3.48 wt% (2.17 mmol/g) at 273K/1bar and 2.21 wt% (1.38 mmol/g) at 298K/1bar, respectively. Obviously, the CH_4 adsorption has not reached saturation in the given pressure range, suggesting that the higher storage can be achieved under higher pressure. The gravimetric uptakes at low pressure for FNOPs-1 is higher than those reported for SNU-C1 (0.67mmol/g),[37] and ILCOF-1 (0.9wt%),[3] and even MOFs (NU-135, ~0.95 mmol/g),[42] but is considerably lower than those of COFs and MOFs obtained at high pressure.[1, 42, 43] The isosteric heats of CH_4 adsorption (Q_{st}) for FNOPs-1 were also calculated by the Virial method (Figure S6B). At zero-coverage, the Q_{st} value for CH_4 uptake is calculated to be 16.35 KJ/mol, which is similar to those reported for various nanoporous organic polymers.[42, 44, 45] The Q_{st} value is lower than that for CO_2 adsorption, indicative of weaker adsorbate-adsorbent interaction in relative to CO_2. However, as shown in Fig.3F, the values first decrease, and then increase with an increase in the adsorption amount. The increasing heat of adsorption indicates the presence of methane-methane attractions.

The CO_2/CH_4 adsorption selectivity calculated from the slopes of the isotherms[21] reach up to 6.15 at 273 K (Figure S7A), which is slightly higher than the corresponding values of MOFs[21] and COFs.[46] The excellent CO_2/CH_4 selectivity of FNOPs-1 can be attributed to the stronger interaction with CO_2 molecule than CH_4. The value is reduced to 3.44 (Figure S7B) with an increase in the temperature at 298K.

Conclusions

In summary, we demonstrated that novel ferrocene-based nanoporous organic polymers (FNOPs-1) has been prepared by coupling 1,1'-ferrocene-dicarboxaldehyde with melamine, and ferrocene was successfully introduced into the network as a building unit. FNOPs-1 exhibited excellent physicochemical and thermal stability, and had a moderate specific surface area (752.4 m^2g^{-1}) and a respectable pore volume (1.32 cm^2/g). Because ferrocene is of withdrawing electron property, FNOPs-1 displayed excellent CO_2 storage capacity (16.61 wt% at 273K/1bar and 11.18 wt% at 298K/1bar), and moderate H_2 and CH_4 uptake at low pressure. The above results suggested that using 1,1'-ferrocene-dicarboxaldehyde as a building unit was a valuable methodology for expanding the porosity of nanoporous organic networks. The present study indicates that the ferrocenyl nanoporous network is a promising candidate as an adsorbent for clean energy application.

Acknowledgements

This work was financially supported by NSFC (Grant 51373051, 51273062, and 51343004), and the Hunan Provincial Natural Science Foundation of China (Grant 14JJ2095, 13JJA004).

References

1. H. Furukawa and O. M. Yaghi, *J. Am. Chem. Soc.*, 2009, **131**, 8875-8883.
2. S. Ding and W. Wang, *Chem. Soc. Rev.*, 2013, **42**, 548-568.
3. M. Rabbani, A. Sekizkardes, Z. Kahveci, T. Reich, R. Ding and H. El-Kaderi, *Chem. Eur. J.*, 2013, **19**, 3324-3328.
4. A. Cooper, *Adv. Mater.*, 2009, **21**, 1291-1295.
5. J. Jiang, F. Su, H. Niu, C. Wood, N. Campbell, Y. Khimyak and A. Cooper, *Chem. Commun.*, 2008, 486-488.
6. N. B. McKeown and P. M. Budd, *Macromolecules*, 2010, **43**, 5163-5176.
7. C. Martin, E. Stockel, R. Clowes, D. Adams, A. Cooper, J. Pis, F. Rubiera and C. Pevida, *J. Mater. Chem.*, 2011, **21**, 5475-5483.
8. Y. Luo, B. Li, W. Wang, K. Wu and B. Tan, *Adv. Mater.*, 2012, **24**, 5703-5707.
9. Y. Luo, B. Li, L. Liang, and B. Tan, *Chem. Commun.*, 2011, **47**, 7704-7706.
10. S. Xiong, X. Fu, L. Xiang, G. Yu, J. Guan, Z. Wang, Y. Du, X. Xiong and C. Pan, *Polym. Chem.*, 2014, **5**, 3424-3431.
11. Y. Liu, S. Wu, G. Wang, G. Yu, J. Guan, C. Pan and Z. Wang, *J. Mater. Chem. A*, 2014, **2**, 7795-7801.
12. S. Wu, Y. Liu, G. Yu, J. Guan, C. Pan, Y. Du, X. Xiong and Z. Wang, *Macromolecules*, 2014, **47**, 2875-2882.
13. R. A. Molla, M. A. Iqubal, K. Ghosh, A. S. Roy, Kamaluddin and S. M. Islam, *RSC Adv.*, 2014, **4**, 48177-48190.
14. M. X. Tan, L. Gu, N. Li, J. Y. Ying and Y. Zhang, *Green Chemistry*, 2013, **15**, 1127-1132.

15. D. S. Zhang, Z. Chang, Y. B. Lv, T. L. Hu and X. H. Bu, *RSC Adv.*, 2012, **2**, 408-410.
16. D. R. van Staveren and N. Metzler-Nolte, *Chem. Rev.*, 2004, **104**, 5931-5986.
17. B. Kiskan and J. Weber, *Polym. Preprints*, 2011, **52**, 865-866.
18. É. Gagnon-Thibault, D. Cossement, R. Guillet-Nicolas, N. Masoumifard, P. Bénard, F. Kleitz, R. Chahine and J.-F. Morin, *Micropor. Mesopor. Mater.*, 2014, **188**, 182-189.
19. S. Ren, R. Dawson, A. Laybourn, J. Jiang, Y. Khimyak, D. Adams and A. Cooper, *Polym. Chem.*, 2012, **3**, 928-934.
20. B. Li, F. Su, H. Luo, L. Liang and B. Tan, *Micropor. Mesopor. Mater.*, 2011, **138**, 207-214.
21. B. Zheng, R. Yun, J. Bai, Z. Lu, L. Du and Y. Li, *Inorg. Chem.*, 2013, **52**, 2823-2829.
22. F. Uribe-Romo, J. Hunt, H. Furukawa, C. Klock, M. O'Keeffe and O. Yaghi, *J. Am. Chem. Soc.*, 2009, **131**, 4570-4571.
23. M. G. Schwab, B. Fassbender, H. W. Spiess, A. Thomas, X. Feng and K. Müllen, *J. Am. Chem. Soc.*, 2009, **131**, 7216-7217.
24. M. K. Bhunia, S. K. Das, P. Pachfule, R. Banerjee and A. Bhaumik, *Dalton Transactions*, 2012, **41**, 1304-1311.
25. D. N. Bunck and W. R. Dichtel, *J. Am. Chem. Soc.*, 2013, **135**, 14952-14955.
26. M. Dogru, A. Sonnauer, A. Gavryushin, P. Knochel and T. Bein, *Chem. Commun.*, 2011, **47**, 1707-1709.
27. Z. Wang, B. Zheng, H. Liu, X. Lin, X. Yu, P. Yi and R. Yun, *Cryst. Growth Des.*, 2013, **13**, 5001-5006.
28. Z. Lu, H. Xing, R. Sun, J. Bai, B. Zheng and Y. Li, *Cryst. Growth Des.*, 2012, **12**, 1081-1084.
29. A. Nagai, X. Chen, X. Feng, X. Ding, Z. Guo and D. Jiang, *Angew. Chem. Int. Ed.*, 2013, **52**, 3770-3774.
30. J. Schmidt, J. Weber, J. Epping, M. Antonietti and A. Thomas, *Adv. Mater.*, 2009, **21**, 702-705.
31. J. Schmidt, M. Werner and A. Thomas, *Macromolecules*, 2009, **42**, 4426-4429.
32. B. Li, R. Gong, Y. Luo and B. Tan, *Soft Matter*, 2011, **7**, 10910-10916.
33. J.-T. Yu, Z. Chen, J. Sun, Z.-T. Huang and Q.-Y. Zheng, *J. Mater. Chem.*, 2012, **22**, 5369-5373.
34. K. T. Jackson, M. G. Rabbani, T. E. Reich and H. M. El-Kaderi, *Polym. Chem.*, 2011, **2**, 2775-2777.
35. Z. Kahveci, T. Islamoglu, G. Shar, R. Ding and H. El-Kaderi, *Crystengcomm*, 2013, **15**, 1524-1527.
36. Q. Chen, M. Luo, P. Hammershøj, D. Zhou, Y. Han, B. W. Laursen, C.-G. Yan and B.-H. Han, *J. Am. Chem. Soc.*, 2012, **134**, 6084-6087.
37. L.-H. Xie and M. P. Suh, *Chem. Eur. J.*, 2013, **19**, 11590-11597.
38. Y. L. Luo, B. Y. Li, W. Wang, K. B. Wu and B. Tan, *Adv. Mater.*, 2012, **24**, 5703-5707.
39. B. S. Zheng, J. F. Bai, J. G. Duan, L. Wojtas and M. J. Zaworotko, *J. Am. Chem. Soc.*, 2011, **133**, 748-751.

40. R. Dawson, D. Adams and A. Cooper, *Chem. Sci.*, 2011, **2**, 1173-1177.
41. W. Lu, D. Yuan, J. Sculley, D. Zhao, R. Krishna and H.-C. Zhou, *J. Am. Chem. Soc.*, 2011, **133**, 18126-18129.
42. R. D. Kennedy, V. Krungleviciute, D. J. Clingerman, J. E. Mondloch, Y. Peng, C. E. Wilmer, A. A. Sarjeant, R. Q. Snurr, J. T. Hupp, T. Yildirim, O. K. Farha and C. A. Mirkin, *Chem. Mater.*, 2013, **25**, 3539-3543.

43. F. Gándara, H. Furukawa, S. Lee and O. M. Yaghi, *J. Am. Chem. Soc.*, 2014, **136**, 5271-5274.

44. C. Wood, B. Tan, A. Trewin, F. Su, M. Rosseinsky, D. Bradshaw, Y. Sun, L. Zhou and A. Cooper, *Adv. Mater.*, 2008, **20**, 1916-1921.

45. G. Barin, V. Krungleviciute, D. A. Gomez-Gualdron, A. A. Sarjeant, R. Q. Snurr, J. T. Hupp, T. Yildirim and O. K. Farha, *Chem. Mater.*, 2014, **26**, 1912-1917.

46. S. Qiao, Z. Du and R. Yang, *J. Mater. Chem. A*, 2014, **2**, 1877-1885.

A Table of Contents Entry

A novel ferrocene-based nanoporous organic polymer has been prepared by coupling 1,1'-ferrocene-dicarboxaldehyde with melamine.

Qingquan Liu[a*], Zhe Tang[a], Minda Wu[a], Bo Liao[a], Hu Zhou[a], Baoli Ou[a], Yu Guipeng[b], Zhihua Zhou[a*], Xiaojuan Li[a]